J|A|C|S ARTICLES

Published on Web 10/16/2009

Mechanism and Plasticity of Isochorismate Pyruvate Lyase: A Computational Study

Sergio Martí,[†] Juan Andrés,[†] Vicent Moliner,*[,†] Estanislao Silla,[‡] Iñaki Tuñón,*[,‡] and Juan Bertrán[§]

Departament de Química Física i Analítica, Universitat Jaume I, 12071 Castellón, Spain, Departament de Química Física, Universitat de València, 46100 Burjasot, Spain, and Departament de Química, Universitat Autònoma de Barcelona, 08193 Bellaterra, Spain

Received June 29, 2009; E-mail: moliner@uji.es; ignacio.tunon@uv.es

Abstract: The isochorismate pyruvate lyase (IPL) from *Pseudomonas aeruginosa*, designated as PchB, catalyzes the transformation of isochorismate into pyruvate and salicylate, but it also catalyzes the rearrangement of chorismate into prephenate, suggesting that both reactions may proceed by a pericyclic mechanism. In this work, molecular dynamics simulations employing hybrid quantum mechanics/molecular mechanics methods have been carried out to get a detailed knowledge of the reaction mechanism of PchB. The results provide a theoretical rate constant enhancement by comparison with the reaction in solution, in agreement with the experimental data, and confirm the pericyclic nature of the reaction mechanism. The robustness of this promiscuous enzyme has been checked by considering the impact of Ala37Ile mutation, previously proposed by us to improve the secondary chorismate mutase (CM) activity. The effect of this mutation, which was shown to increase the rate constant for the CM activity by a factor of 10^3, also increases the IPL catalytic efficiency, although only by a factor of 6.

Introduction

Traditionally, pericyclic reactions have been considered as a rarely exploited mechanism in cellular metabolism, despite their broad utility in the laboratory.[1] In fact, just a few examples of this kind of reaction have been considered to be catalyzed by enzymes, including the Claisen rearrangement of chorismate to prephenate,[2] the suprafacial [1,5] sigmatropic shift of a methyl group in the transformation of precorrin-8x to hydrogenobyrinic acid,[3] and several putative Diels−Alder reactions.[4] Nevertheless, the catalytic mechanism of some pyruvate lyases, initially described as a general base process,[5] has recently been proposed to follow a concerted pericyclic pathway.[1,6−8] Thus, in the elimination of the enolpyruvyl side chain from isochorismate to give salicylate and pyruvate catalyzed by the enzyme PchB,[6,9] the hydrogen atom would be transferred to the carbon atom of the side chain simultaneously with carbon−oxygen cleavage (Figure 1a).[1,7,8] Moreover, several authors have recently suggested that other enzymes belonging to the MST enzyme family, such as MbtI[10,11] and Irp9,[12,13] could also follow this kind of mechanism.

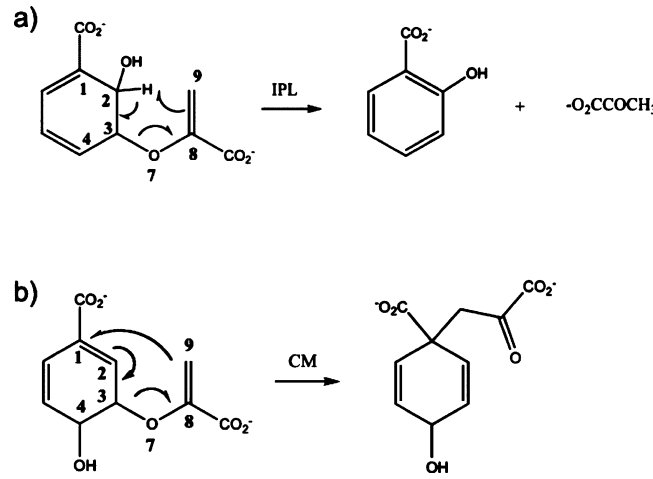

Figure 1. Schematic diagrams illustrating the transformations of (a) isochorismate to salicylate and pyruvate and (b) chorismate to prephenate.

In the case of PchB, salicylate is essential in the biosynthesis of siderophores, low-molecular-mass organic ferric chelators that

[†] Universitat Jaume I.
[‡] Universitat de València.
[§] Universitat Autònoma de Barcelona.

(1) DeClue, M. S.; Baldridge, K. K.; Künzler, D. R.; Kast, P.; Hilvert, D. *J. Am. Chem. Soc.* **2005**, *127*, 15002.
(2) Chook, Y. M.; Ke, H.; Lipscomb, W. N. *Proc. Natl. Acad. Sci. U.S.A.* **1993**, *90*, 8600.
(3) Li, Y.; Alanine, A. I. D.; Vishwakarma, R. A.; Balachandran, S.; Leeper, F. J.; Battersby, A. R. *Chem. Commun.* **1994**, 2507.
(4) Stocking, E. M.; Williams, R. M. *Angew. Chem., Int. Ed.* **2003**, *42*, 3078.
(5) Walsh, C. T.; Liu, J.; Rusnak, F.; Sakaitani, M. *Chem. Rev.* **1990**, *90*, 1105.
(6) (a) Zaitseva, J.; Lu, J.; Olechoski, K. L.; Lamb, A. L. *J. Biol. Chem.* **2006**, *281*, 33441. (b) Luo, O.; Olucha, J.; Lamb, A. L. *Biochemistry* **2009**, *48*, 5239.
(7) Künzler, D. E.; Sasso, S.; Gamper, M.; Hilvert, D.; Kast, P. *J. Biol. Chem.* **2005**, *280*, 32827.
(8) DeClue, M. S.; Baldridge, K. K.; Kast, P.; Hilvert, D. *J. Am. Chem. Soc.* **2006**, *128*, 2043.
(9) Gaille, C.; Kast, P.; Haas, D. *J. Biol. Chem.* **2002**, *277*, 21768.
(10) Harrison, A. J.; Yu, M.; Gardenborg, T.; Middleditch, M.; Ramsay, R. J.; Baker, E. N.; Lott, J. S. *J. Bacteriol.* **2006**, *188*, 6081.
(11) Zwahlen, J.; Subramaniapillai, K.; Zhou, R.; Kisker, C.; Tonge, P. J. *Biochemistry* **2007**, *46*, 954.

10.1021/ja905271g CCC: $40.75

are used by pathogenic bacteria to get iron from the hosts' stores to support their metabolism.[12] Otherwise, salicylic acid mediates plant defenses against pathogens, including both local and systematic acquired resistance.[14] In fact, production of salicylic acid in plants by bacterial transgenes has been proposed as an efficient strategy for improving their resistance.[15] Knowledge of the reaction mechanism is the keystone for computer-guided production of more efficient enzymatic inhibitors that could result in new and potent weapons against resistant bacteria.

In order to demonstrate the pericyclic mechanism of PchB, various techniques such as deuterium isotopic labeling to study kinetic isotope effects (KIEs), site-directed mutagenesis, and theoretical calculations in the gas phase have been employed by Hilvert and co-workers for the catalyzed[1,7] and uncatalyzed reactions.[8] In view of the impact that this new hypothesis has received in the proposal of similar mechanisms for other enzymes, the first aim of the present study was to test the hypothesis that the isochorismate pyruvate lyase (IPL) reaction of PchB is indeed pericyclic. Moreover, our computing methods have allowed us to obtain more detailed information about the timing of the forming and breaking bonds as well as a molecular level description of the enzyme effects, affording deep insight into the reaction catalyzed by PchB. The results will show whether the reaction can proceed by means of a pericyclic mechanism and, moreover, whether the enhancement of the rate constant deduced from this mechanism, by comparison with the reaction in solution, is in agreement with the experimental data.

Analysis of the apo and pyruvate-bound X-ray structures of PchB[6] revealed no sequence similarity to other pyruvate lyases that traditionally have been accepted to act through a general base mechanism.[5] Instead, PchB shares 20% sequence identity with the chorismate mutases (CMs) of the AroQ family, a subclass that uses a Claisen rearrangement mechanism (Figure 1b).[6,9] The quaternary structure of PchB was found to be dimeric, as it is for *Escherichia coli* CM (EcCM), and most of the catalytic residues of EcCM are conserved in PchB. Thus, it is not surprising that PchB also presents secondary activity catalyzing the transformation of chorismate into prephenate.[9] This promiscuity would be in agreement with the proposed pericyclic mechanism for PchB.[1,6,7] More recently, and in agreement with these ideas, the fact that MbtI[10,11] and Irp9[13] also present a certain catalytic efficiency with respect to the chorismate-to-prephenate rearrangement (which is broadly accepted to proceed by a [3,3]-sigmatropic pericyclic rearrangement) has been invoked to suggest that the reaction mechanism of its primary reaction, conversion of chorismate to salicylate, can also be catalyzed by these enzymes via a pericyclic mechanism.

Enzyme promiscuity of PchB in catalyzing the chorismate-to-prephenate rearrangement has been the source of inspiration to convert a CM into an IPL. Nevertheless, not a trace of this activity has been detected in CM variants mutated to more closely resemble the IPL active site.[16] On the other hand, we recently carried out a theoretical study that predicted a selected mutation of the enzyme active site of PchB that would improve the secondary activity.[17] In particular, we found that the Ala37Ile mutation would reduce the free-energy barrier of the chorismate-to-prephenate rearrangement by 4.4 kcal mol^{-1}, showing the plasticity of PchB,[18−22] where plasticity is defined as the ability of few or even a single engineered mutation to increase the promiscuous activity by orders of magnitude. Promiscuous enzymes show plasticity, but also, as pointed out by Tawfik and co-workers,[22] in many cases improvements in promiscuous functions do not seem to be accompanied by parallel decreases in the original function. It appears that proteins exhibit both plasticity and robustness.[21,22] This feature is believed to be essential for the evolution of new enzymatic activities. While the traditional model of Ohno[23] assumes that the new function appears on a duplicated gene, which is free to accumulate mutations without selective pressure, in current gene-sharing models a gene with a function is recruited for a new one before duplication, assuming that the gene possesses secondary or promiscuous activity that can be improved without a significant loss of the original function.[24]

In this paper, we will present the first theoretical proof of the reaction mechanism of the transformation of isochorismate to give salicylate and pyruvate in the active site of wild-type PchB, compared with the same reaction in solution. For this purpose, a hybrid quantum mechanics/molecular mechanics (QM/MM) scheme[25] has been used to carry out molecular dynamics (MD) simulations to study the complete chemical reaction including the dynamics of the full system.[26] Afterward, we will explore the robustness of this promiscuous enzyme under the Ala37Ile mutation, previously proposed by us to improve its secondary activity,[17] by analyzing the impact on the primary function. The results provide further evidence that computational investigation of the active sites of enzymes with known structures is a valid starting point for direct enzyme engineering through exploitation of promiscuous activities.

Computational Methods

Our analysis started with the X-ray structure of PchB (Protein Data Bank entry 2H9D)[6a] containing two pyruvate molecules into the active site. The original substrates were replaced by the gas-phase transition-state (TS) structure of the rearrangement. The "cluster method"[27,28] was used to recalculate the standard pK_a values of the titratable amino acids of the enzyme. The hydrogen atoms were incorporated into the structure using fDYNAMO.[29] Next, sodium counterions were added to neutralize the total charge. The resulting system was placed in a simulation water box with side lengths of 79.5 Å, and any water molecule having an oxygen

(12) Kerbarh, O.; Chirgadze, D. Y.; Blundell, T. L.; Abell, C. *J. Mol. Biol.* **2006**, *357*, 524.
(13) Kerbarh, O.; Ciulli, A.; Chirgadze, D. Y.; Blundell, T. L.; Abell, C. J. *ChemBioChem* **2007**, *8*, 622.
(14) Wildermuth, M. C.; Dewdney, J.; Wu, G.; Ausubel, F. M. *Nature* **2001**, *414*, 562.
(15) Verbene, M. C.; Verpoorte, R.; Bol, J. F.; Mercado-Blanco, J.; Linthorst, H. J. M. *Nat. Biotechnol.* **2008**, *18*, 779.
(16) Jäckel, C.; Kast, P.; Hilvert, D. *Annu. Rev. Biophys.* **2008**, *37*, 153.
(17) Martí, S.; Andrés, J.; Moliner, V.; Silla, E.; Tuñón, I.; Bertrán, J. *J. Am. Chem. Soc.* **2008**, *130*, 2894.
(18) Toscano, M. D.; Woycechowsky, K. J.; Hilvert, D. *Angew. Chem., Int. Ed.* **2007**, *46*, 3212.
(19) O'Brien, P. J.; Herschlag, D. *Chem. Biol.* **1999**, *6*, R91.
(20) Copley, S. D. *Curr. Opin. Chem. Biol.* **2003**, *7*, 265.
(21) Aharoni, A.; Gaidukov, L.; Khersonsky, O.; Gould, S. M.; Roodveldt, C.; Tawfik, D. S. *Nat. Genet.* **2005**, *37*, 73.
(22) Khersonsky, O.; Roodveldt, C.; Tawfik, D. S. *Curr. Opin. Chem. Biol.* **2006**, *10*, 498.
(23) Ohno, S. *Evolution by Gene Duplication*; Springer: New York, 1970.
(24) McLoughlin, S. Y.; Copley, S. D. *Proc. Natl. Acad. Sci. U.S.A.* **2008**, *105*, 13497.
(25) Warshel, A.; Levitt, M. *J. Mol. Biol.* **1976**, *103*, 227.
(26) Roca, M.; Martí, S.; Andrés, J.; Moliner, V.; Silla, E.; Tuñón, I.; Bertrán, J. *Chem. Soc. Rev.* **2004**, *33*, 98.
(27) Antosiewicz, J.; McCammon, J. A.; Gilson, M. K. *J. Mol. Biol.* **1994**, *238*, 415.
(28) Field, M.; David, L.; Rinaldo, D. Personal communication, 2006.
(29) Field, M. J.; Albe, M.; Bret, C.; Proust-de Martin, F.; Thomas, A. J. *J. Comput. Chem.* **2000**, *21*, 1088.

atom lying within a radius of 2.8 Å from any non-hydrogen atom was removed.

The substrate was described using QM at the AM1 level,[30] while for the rest of the system, we used MM with the OPLS-AA[31] and TIP3P[32] force fields. Periodic boundary conditions were employed in combination with a switched cutoff radius of 14.5 to 16 Å for the nonbonded interactions. The full system was relaxed by successive QM/MM minimization steps using a micro−macro iterations approach.[33] The system was then equilibrated at 300 K using the NVT ensemble and the Langevin−Verlet integrator with a time step of 1.0 fs during a total time of 500 ps, during which the geometry of the substrate was maintained close to the TS structure by means of harmonic restraints applied to internal coordinates. To study the chemical reaction in solution, we used a similar protocol, placing the QM subsystem in a 55.8 Å side length box of TIP3P water molecules.

Catalytic activity is usually discussed in the context of transition state theory (TST),[34] which analyzes the effect on the activation free energy in comparison with the counterpart process in aqueous solution.[26] Our approach was to estimate the activation free energy from the potential of mean force (PMF) $W(\xi)$ obtained as a function of a distinguished reaction coordinate ξ. The PMF is related to the normalized probability of finding the system at a particular value of the chosen coordinate, as shown in eq 1:

$$W(\xi) = C - kT \ln \int \rho(\mathbf{r}^N)\, \delta(\xi(\mathbf{r}^N) - \xi)\, \mathrm{d}\mathbf{r}^{N-1} \qquad (1)$$

The activation free energy can be then expressed as:[35]

$$\Delta G^{\ddagger}(\xi) = W(\xi^{\ddagger}) - [W(\xi^{\mathrm{R}}) + G_{\xi}(\xi^{\mathrm{R}})] \qquad (2)$$

where the ‡ and R superscripts indicate the value of the reaction coordinate at the TS and reactants, respectively, and $G_{\xi}(\xi^{\mathrm{R}})$ is the free energy associated with setting the reaction coordinate to a specific value in the reactant state. Normally this last term makes only a small contribution,[36] so the activation free energy is directly estimated from the PMF change between the maximum in the free-energy profile and the reactant minimum:

$$\Delta G^{\ddagger}(\xi) \approx W(\xi^{\ddagger}) - W(\xi^{\mathrm{R}}) = \Delta W^{\ddagger}(\xi) \qquad (3)$$

The selection of the reaction coordinate is usually trivial when the mechanism is driven by a single internal coordinate or a simple combination (e.g., the antisymmetric combination of two interatomic distances). However, this is not the case for the IPL-catalyzed reaction. The reaction can be described as breaking of the bond between the C3 and O7 atoms and a hydrogen transfer from C2 to C9. All attempts to use a single internal coordinate or a combination of them failed to produce a smooth free-energy profile. Instead, we were compelled to obtain a much more computationally demanding two-dimensional PMF (2D-PMF) using two coordinates: the C3−O7 distance (ζ_1) and the antisymmetric combination of the C2−H and C9−H distances (ζ_2). The 2D-PMF is related to the probability of finding the system at particular values of these two coordinates:

$$W(\zeta_1, \zeta_2) = C' - kT \ln \int \rho(\mathbf{r}^N)\, \delta(\zeta_1(\mathbf{r}^N) - \zeta_1)\, \delta(\zeta_2(\mathbf{r}^N) - \zeta_2)\, \mathrm{d}\mathbf{r}^{N-2} \qquad (4)$$

To estimate the activation free energy from this quantity, we recovered one-dimensional PMF changes by tracing a maximum-probability reaction path on the 2D-PMF surface and integrating over the perpendicular coordinate.

The 2D-PMFs corresponding to the reactions in aqueous solution, the native enzyme, and the mutated form were obtained using the weighted histogram analysis method (WHAM) combined with the umbrella sampling approach.[37,38] Simulations were performed at different values of ζ_2 (40 simulations in a range from −1.5 to 2.5 Å with an umbrella force constant of 2800 kJ mol^{-1} A^{-1}) for each value of ζ_1 (eight simulations in a range from 1.3 to 2.2 Å with a force constant of 2500 kJ mol^{-1} A^{-1}). Consequently, there were 320 windows per 2D-PMF. In each window, 5 ps of relaxation was followed by 10 ps of production with a time step of 0.5 fs. The values of the variables sampled during the simulations were then pieced together to construct a full distribution function, from which the 2D-PMFs were obtained.

Because of the large number of structures that must be evaluated during free-energy calculations, QM/MM calculations are usually restricted to the use of semiempirical Hamiltonians such as the AM1 Hamiltonian. In order to reduce the errors associated with the level of quantum theory employed in our simulations, we used a new energy function defined in terms of interpolated corrections, as shown in eq 5:[39−41]

$$E = E_{\mathrm{AM1/MM}} + S[\Delta E^{\mathrm{HL}}_{\mathrm{LL}}(\zeta_1, \zeta_2)] \qquad (5)$$

where S denotes a two-dimensional spline function whose argument $\Delta E^{\mathrm{HL}}_{\mathrm{LL}}(\zeta_1, \zeta_2)$ is a correction term evaluated as the gas-phase difference between a high-level (HL) energy of the QM subsystem and the low-level (LL) result (AM1 in this case). The B3LYP/6-31G** level of theory[42,43] was used to perform the HL calculations. These calculations were carried out using the *Gaussian03* program.[44]

Results

In this section, the results for the enzyme reaction mechanism of the PchB-catalyzed transformation from isochorismate to salicylate and pyruvate, compared with the reference reaction in solution, will be presented first, and then the study of the effect of Ala37Ile mutation on the protein catalytic efficiency will be discussed.

Reaction Mechanism in PchB. The B3LYP/MM 2D-PMFs for the elimination of the enolpyruvyl side chain from isochorismate to give salicylate and pyruvate obtained in the enzyme and in solution are displayed in Figure 2. As can be observed, the reaction takes place in a concerted but very asynchronous way in both media. The reaction paths traced on the free-energy surfaces show that the reaction proceeds first through a C3−O7 bond lengthening from ∼1.5 to ∼1.9 Å, and from this structure, the reaction then proceeds essentially as a hydrogen transfer

(30) Dewar, M. J. S.; Zoebisch, E. G.; Healy, E. F.; Stewart, J. J. P. *J. Am. Chem. Soc.* **1985**, *107*, 3902.
(31) Jorgensen, W. L.; Maxwell, D. S.; Tirado-Rives, J. *J. Am. Chem. Soc.* **1996**, *118*, 11225.
(32) Jorgensen, W. L.; Chandrasekhar, J. M.; Madura, J. D.; Impey, R. W.; Klein, M. L. *J. Chem. Phys.* **1983**, *79*, 926.
(33) Martí, S.; Moliner, V.; Tuñón, I. *J. Chem. Theory Comput.* **2005**, *1*, 1008.
(34) Eyring, H. *J. Chem. Phys.* **1935**, *3*, 107.
(35) Schenter, G. K.; Garrett, B. C.; Truhlar, D. G. *J. Chem. Phys.* **2003**, *119*, 5828.
(36) Roca, M.; Moliner, V.; Ruiz-Pernía, J. J.; Silla, E.; Tuñón, I. *J. Phys. Chem. A* **2006**, *110*, 503.
(37) Kumar, S.; Bouzida, D.; Swendesen, R. H.; Kollman, P. A.; Rosemberg, J. M. *J. Comput. Chem.* **1992**, *13*, 1011.
(38) Torrie, G. M.; Valleau, J. P. *J. Comput. Phys.* **1977**, *23*, 187.
(39) Ruiz-Pernía, J. J.; Silla, E.; Tuñón, I.; Martí, S.; Moliner, V. *J. Phys. Chem. B* **2004**, *108*, 8427.
(40) Roca, M.; Moliner, V.; Ruiz-Pernía, J. J.; Silla, E.; Tuñón, I. *J. Phys. Chem. A* **2006**, *110*, 503.
(41) Chuang, Y. Y.; Corchado, J. C.; Truhlar, D. G. *J. Phys. Chem. A* **1999**, *103*, 1140.
(42) Becke, A. D. *Phys. Rev. A* **1988**, *38*, 3098.
(43) Lee, C.; Yang, W.; Parr, R. G. *Phys. Rev. B* **1988**, *37*, 785.
(44) Frisch, M. J.; et al. *Gaussian 03*; Gaussian, Inc.: Pittsburgh, PA, 2003.

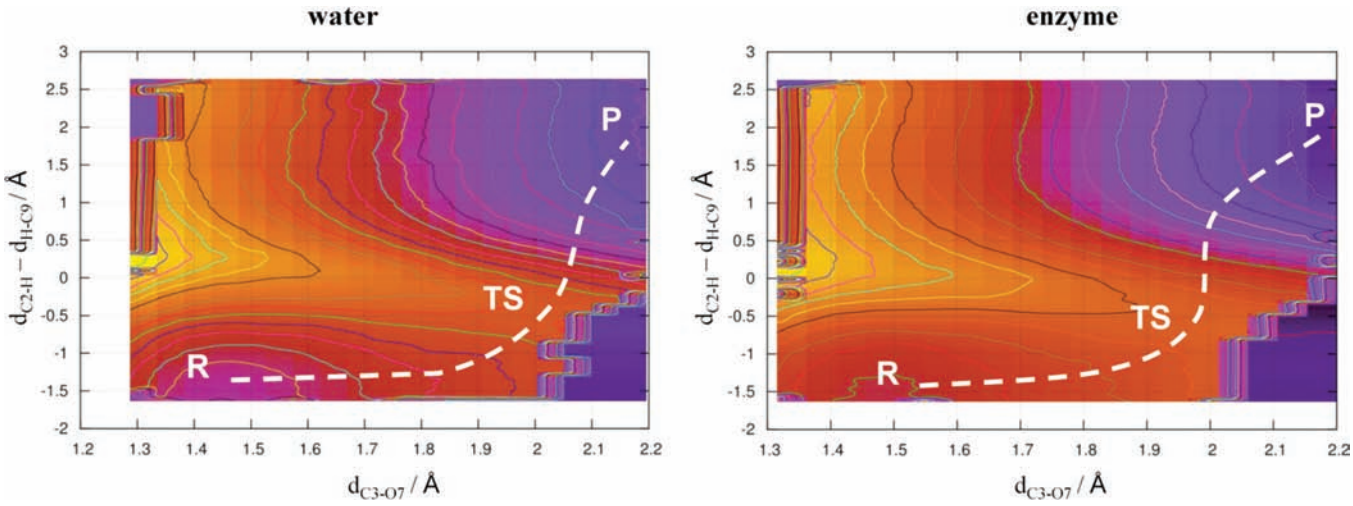

Figure 2. 2D-PMFs obtained at 278 K. The distinguished reaction coodinates are the C3−O7 distance (d_{C3-O7}) and the antisymmetric combination of the breaking and forming bonds of the transferred hydrogen atom, $d_{C2-H} - d_{H-C9}$. Isoenergetic lines are drawn every 5 kcal mol^{-1}. Purple regions correspond to the minima, while yellow color represents higher energies on the surface. Reaction paths are shown as white dashed lines.

Table 1. Free-Energy Barriers in Terms of Changes in Potential of Mean Force (ΔPMF) Computed at the B3LYP Level Along with Experimental Values ($\Delta G^{\ddagger}_{exptl}$) in kcal mol^{-1}

	$\Delta PMF^{\ddagger}_{AM1/MM}$	$\Delta PMF^{\ddagger}_{B3LYP/MM}$	$\Delta G^{\ddagger}_{exptl}$
PchB	38.4	17.9	17.7[a]
water	43.1	25.9	26.2[b]
$\Delta\Delta^{\ddagger}$	4.7	8.0	8.5

[a] Calculated using data at 30 °C from ref 9. [b] Calculated using data at 60 °C from ref 8.

from C2 to C9 to reach the TS. Once they arrive at the TS, the paths continue on to products to complete the hydrogen transfer, with a last stage where the C3−O7 distance lengthens slightly. This behavior is not chemically unexpected, since the heterolytic cleavage of the carbon−oxygen bond generates a negatively charged enolpyruvyl side chain and a positively charged ring, which favors the proton transfer from C2 to C9 (see below).

From the energetic point of view, the activation free energies are very close to the experimental values, and as the data in Table 1 show, the enzyme reduces the free-energy barrier by 8.0 kcal mol^{-1}. These results are in very good agreement with the experimental data. It must be pointed out that the experimental data were obtained by applying TST to the experimental first-order rate constants obtained at 30 °C for the enzyme reaction and 60 °C for the solution reaction. This agreement between the experimental data and theoretical predictions supports the herein proposed pericyclic mechanism previously suggested by Hilvert and co-workers.[1,7,8] Moreover, we can be confident in our calculations, and a deeper analysis into the molecular mechanism can be carried out in order to explain the source of the enzyme catalytic role.

Average values of the key geometrical parameters of the substrate located in the active site of PchB and in solution, in both R and the TS, are listed in Table 2, and structures are depicted in Figure 3. Analysis of the results reveals that both the C−O bond breaking and the proton transfer are more advanced in the TS for the reaction in solution than in the TS for the enzyme-catalyzed reaction. Furthermore, the distance between the two carboxylate groups is longer in solution than in the enzyme (see the $d_{CO_2^-}-_{CO_2^-}$ distance in Table 2). The conformations found in solution are dominated by the electrostatic interaction between the two carboxylate groups. In the enzyme, this distance is shorter and hardly changes in going from R to the TS, thus suggesting that the energy penalty associated with the electrostatic repulsion between these groups is compensated by intermolecular interactions with residues of the active site. These differences in the distance between the two carboxylate groups cause preferences for different substrate conformations in the enzyme and in solution. Effectively, with respect to the relative orientation of the carboxylate group of the enolpyruvyl side chain and the ring, the substrate conformations could be classified as endo or exo conformations. In terms of this classification, the reaction in the aqueous medium takes place through an exo conformation, which is in agreement with the gas-phase potential energy profiles studied by Hilvert and co-workers,[8] while endo conformers are found in the enzyme active site. The endo conformations result in a chairlike TS, while the exo conformations result in a twist−boat TS (Figure 3).

Table 2. Average Values of Key Geometrical Parameters [Distances (*d*) in Å, Angles (*a*, *z*) in deg] for Reactants (R) and Transition State (TS) Obtained in PchB and in Aqueous Solution from 2D-PMFs Computed at the B3LYP/MM Level

	enzyme		water	
	R	TS	R	TS
d_{C3-O7}	1.461 ± 0.037	1.949 ± 0.013	1.439 ± 0.028	2.016 ± 0.015
d_{H-C2}	1.132 ± 0.029	1.236 ± 0.032	1.134 ± 0.030	1.293 ± 0.033
d_{H-C9}	2.591 ± 0.141	1.757 ± 0.034	2.909 ± 0.433	1.591 ± 0.034
$d_{C2-H} - d_{H-C9}$	−1.459 ± 0.143	−0.512 ± 0.016	−1.776 ± 0.433	−0.298 ± 0.017
$a_{C2-H-C9}$	129.4 ± 5.9	151.5 ± 5.8	109.1 ± 8.2	152.7 ± 5.9
$d_{CO_2^-}-_{CO_2^-}$	5.405 ± 0.168	5.399 ± 0.151	6.880 ± 0.230	5.999 ± 0.195
$z_{C4-C3-C8-C9}$	−152.23 ± 7.50	−141.87 ± 5.12	−52.23 ± 12.04	−86.15 ± 7.86
$d_{OH-CO_2^-}$	2.191 ± 0.168	2.129 ± 0.160	2.691 ± 0.617	2.224 ± 0.312

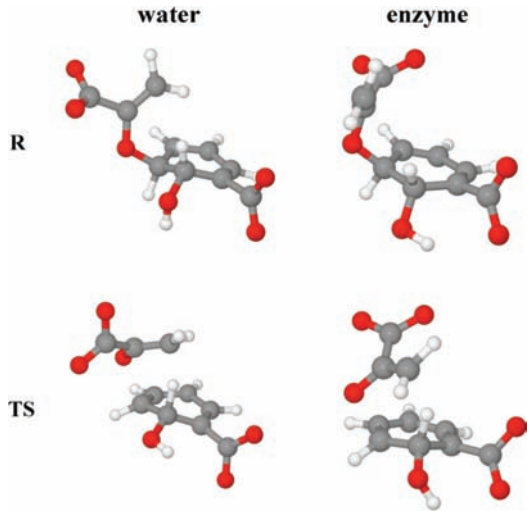

Figure 3. Representative structures of the substrate in the reactant (R) and transition state (TS) in aqueous solution (water) and PchB (enzyme).

The reaction can be also studied from the electronic point of view by analyzing the evolution of the Mulliken charges in going from R to the TS. To simplify the discussion, the charge separation between species resulting from heterolytic cleavage of the C−O bond, which ideally would lead to an enolpyruvyl side chain of charge −2 and a remaining neutral species, have been computed. After cleavage of the C−O bond, the subsequent proton transfer would obviously produce products in the final stage. The charge separation between these two fragments increases in going from R to the TS in both the enzyme (from −0.429 to −0.859 au) and solution (from −0.337 to −0.761 au). However, and this is the important point, the enzyme polarizes the substrate, favoring the charge separation and the subsequent proton transfer. Obviously, the polarization is related to the geometrical changes discussed above and to intermolecular interactions between the substrate and the protein.

Figure 4 shows a snapshot of the TS obtained in the enzyme active site, and distances for the most important substrate−protein interactions in R and the TS are listed in Table 3. Analysis of the results shows that the oxygen atom involved in bond breaking interacts with Lys42 and Gln90, polarizing the C−O bond and favoring the heterolytic cleavage. The carboxylate group of the enolpyruvyl side chain interacts favorably with Arg14 and Arg53, while the carboxylate of the ring interacts with Arg31 and Arg53. It is important to point out that Glu89, which has been previously proposed as the residue that extracts the proton in a general base mechanism,[5] is more than 11 Å away from the substrate (Table 3), thus also supporting the proposed pericyclic mechanism.

PchB Enzyme Plasticity. As mentioned in the Introduction, we recently carried out a theoretical study whose results predicted that the Ala37Ile mutation of the enzyme active site of PchB would improve its secondary activity.[17] In particular, this mutation reduces the free-energy barrier of the chorismate-to-prephenate rearrangement by 4.4 kcal mol^{-1} by keeping the enolpyruvyl side chain closer to the ring in the reactants, thus favoring the diaxial character required for the TS of a pericyclic reaction. Within the context of the shared gene theory, a mutation of the enzyme that improves the secondary catalytic activity should not dramatically affect the primary reaction efficiency (i.e., it should be a neutral mutation). The purpose of this section is to study the primary reaction of the mutated PchB enzyme, for which the mutation was observed to improve the secondary reaction, the conversion from chorismate to prephenate. It is important to note that this mutation gives two possible stable rotamers of the isochorismate, depending on the orientation of the Ile37 residue. Starting from these two conformers, two different free-energy surfaces were obtained with respect to the two rotamers revealed as stable during the reaction. The resulting two surfaces are qualitatively identical to the one calculated for the wild-type enzyme (Figure 2), and the activation free energies deduced from them (16.0 and 16.8 kcal mol^{-1}) are almost equal within the statistical uncertainty. Interestingly, the Ala37Ile mutation not only fails to increase the free-energy barrier but actually decreases by at least 1.1 kcal mol^{-1} the barrier obtained for the wild-type enzyme (Table 1). Representative snapshots corresponding to R and TS located on the free-energy surfaces for the native and Ala37Ile-mutated enzymes are depicted in Figure 4. Figure 4 and Table 3 reveal that the steric effect of this mutation keeps the enolpyruvyl side chain closer to the ring, thus moving the proton closer to the acceptor carbon atom and decreasing the barrier of the proton transfer. This effect can be monitored by measuring the distance

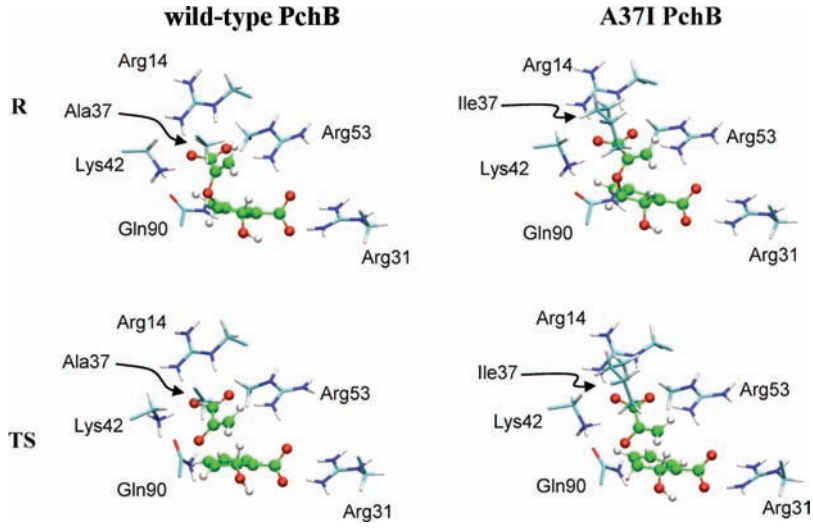

Figure 4. Detailed structures of the reactant (R) and transition state (TS) obtained in the active sites of the wild-type PchB and A37I PchB mutated enzymes together with key amino acids of the active sites.

Table 3. Averaged Intermolecular Substrate−Protein Distances (in Å) and Active-Site Volumes (in Å^3) for Reactants (R) and Transition State (TS) Obtained in Wild-Type PchB and the A37I PchB Mutant

	wild-type PchB		A37I PchB	
	R	TS	R	TS
Arg14−O15	1.850 ± 0.122	2.009 ± 0.151	1.806 ± 0.104	1.881 ± 0.117
Arg14−O16	1.807 ± 0.111	1.764 ± 0.108	1.764 ± 0.098	1.744 ± 0.098
Arg31−O12/O13	1.750 ± 0.101	1.759 ± 0.102	1.782 ± 0.107	1.779 ± 0.104
Lys42−O7	2.424 ± 0.219	2.247 ± 0.161	2.502 ± 0.219	2.216 ± 0.164
Arg53−O12/O13	1.946 ± 0.174	1.942 ± 0.155	1.957 ± 0.161	1.980 ± 0.176
Arg53−O15/O16	2.023 ± 0.177	1.961 ± 0.156	2.005 ± 0.177	1.966 ± 0.163
Glu89−H	11.927 ± 0.329	12.215 ± 0.251	11.580 ± 0.293	12.172 ± 0.269
Gln90−O7	1.878 ± 0.125	1.901 ± 0.129	1.863 ± 0.114	1.837 ± 0.114
CB Ala37-C1	7.719 ± 0.263	7.658 ± 0.291	−	−
CG Ile37−C1	−	−	7.404 ± 0.228	7.378 ± 0.170
active-site volume	344.7 ± 15.4	346.4 ± 11.0	317.8 ± 16.3	309.9 ± 15.5

between the methyl carbon atoms of the amino acid side chains (the CB and CG atoms of Ala37 and Ile37, respectively) and the C1 atom of the substrate. The mutation of the original residue to a larger one also causes a reduction in the volume of the active site in going from the native to the mutant in both the reactants and the TS. All in all, the observed qualitative effect on the primary reaction is similar to the one producing the enhancement in the rate constant for the secondary reaction.[17]

Conclusions

MD simulations employing hybrid QM/MM methods have been carried out to obtain detailed knowledge of the molecular mechanism for the PchB-catalyzed elimination of the enolpyruvyl side chain from isochorismate to give salicylate and pyruvate. For this purpose, 2D-PMFs were computed at 300 K for the catalyzed reaction, and the same protocol was repeated for the reaction in aqueous solution. Our theoretical simulations demonstrate that the primary reaction catalyzed by PchB takes place by a pericyclic mechanism, which, despite being quite common in organic synthesis, is considered rare in enzyme catalysis.[1] Moreover, the enhancement of the rate constant in comparison with the reaction in solution is in agreement with the experimental data; our predicted decrease in the free-energy barrier of the catalyzed reaction is 8.0 kcal mol^{-1}, while an experimental free-energy lowering of 8.5 kcal mol^{-1} can be deduced from the data obtained by Gaille et al.[9] and by DeClue et al.[8]

Once the molecular mechanism of the PchB primary reaction was established, the plasticity of this promiscuous enzyme was studied in regard to the impact of the Ala37Ile mutation, which was previously proposed by us to improve its secondary activity.[17] The theoretical prediction is that this mutation decreases the free-energy barrier of the native PchB primary reaction from 17.9 to 16.8 kcal mol^{-1}. This means that PchB is robust against Ala37Ile mutation, and the amazing result is that the increase in the activity of the mutant enzyme for the secondary reaction by a factor of 10^3 (CM activity)[17] is accompanied by a small but favorable change in the primary reaction (IPL activity), increasing k_{cat} by a factor of 6.3 at 300 K. Although this mutation has not been carried out to date, Mayo and co-workers[45] have performed several mutations of *E. coli* chorismate mutase and evaluated their effects on its primary reaction, the chorismate-to-prephenate rearrangement. From the experimental data reported on the tested mutations,[45] two of them could be combined to be considered equivalent to a hypothetical Ala37Ile mutation, with a rate constant enhancement by a factor of 3.2.

This study shows how the structure of the active sites of existing enzymes can provide a starting point for engineering novel enzymes with new or more efficient catalytic functions, thus paving the way for a potent computational protocol to assist molecular engineering.

Acknowledgment. This work was supported by DGI Project CTQ2006-15447-C02-01/BQU, BANCAIXA Projects P1·1B2008-38 and P1·1B2008-36, and Generalitat Valenciana Projects GV06/152 and GV06/21. We acknowledge the Servei d'Informàtica of the Universitat Jaume I and the Barcelona Supercomputer Center for providing us with computer capabilities. We thank Dr. A. L. Lamb for kindly providing us the X-ray structure of PchB.

Supporting Information Available: Complete ref 44. This material is available free of charge via the Internet at http://pubs.acs.org.

JA905271G

(45) Lassila, J. K.; Keeffe, J. R.; Kast, P.; Mayo, S. L. *Biochemistry* **2007**, *46*, 6883.